Biochemical and Biophysical Research Communications 691 (2024) 149286

Contents lists available at ScienceDirect

Biochemical and Biophysical Research Communications

journal homepage: www.elsevier.com/locate/ybbrc

Prevention of vincristine-induced peripheral neuropathy by protecting the endothelial glycocalyx shedding

Kazufumi Ohmura [a,b,1], Takamasa Kinoshita [c,1], Hiroyuki Tomita [b,d,*], Hideshi Okada [d,e,**], Masayoshi Shimizu [b], Kosuke Mori [b], Toshiaki Taniguchi [b], Akio Suzuki [f], Toru Iwama [a], Akira Hara [b]

[a] Department of Neurosurgery, Gifu University Graduate School of Medicine, Gifu, Japan
[b] Department of Tumor Pathology, Gifu University Graduate School of Medicine, Gifu, Japan
[c] Department of Neurosurgery, Ogaki Tokusyukai Hospital, Gifu, Japan
[d] Center for One Medicine Innovative Translational Research, Gifu University Institute for Advanced Study, Gifu, Japan
[e] Department of Emergency and Disaster Medicine, Gifu University Graduate School of Medicine, Gifu, Japan
[f] Department of Pharmacy, Gifu University Hospital, Gifu, Japan

ARTICLE INFO

Keywords:
Vincristine-induced peripheral neuropathy
Endothelial glycocalyx
Blood–nerve barrier

ABSTRACT

Vincristine-induced peripheral neuropathy (VIPN) adversely affects the quality of life and treatment continuity of patients. The endothelial glycocalyx (eGCX) protects nerves from harmful substances released from the capillary vessels, but its role in peripheral neuropathy remains unclear. We investigated the impact of eGCX protection on VIPN. Using a murine model of VIPN, we administered nafamostat mesylate to protect the eGCX shedding, and analyzed the eGCX integrity and manifestation of peripheral neuropathy. Nafamostat treatment suppressed allodynia associated with neuropathy. Additionally, nafamostat administration resulted in the suppression of increased vascular permeability in capillaries of peripheral nerves, further indicating its positive influence on eGCX in VIPN model mice. This study provided the importance of eGCX in VIPN. With the potential for rapid clinical translation through drug repositioning, nafamostat may be a new promising treatment for the prevention of VIPN.

1. Introduction

Vincristine-induced peripheral neuropathy (VIPN) is a well-known side effect of vincristine [1]. The mechanism of VIPN remains unclear, and there is no definitive prevention or effective treatment [2]. Therefore, if VIPN occurs, it poses a serious challenge to the treatment of cancer patients. For example, the appearance of VIPN affects drug dosage and drug selection during chemotherapy, and in severe cases, chemotherapy with vincristine is difficult and requires drug withdrawal [1]. Furthermore, cases of VIPN often have incomplete recovery, which adversely affects the quality of life of patients even after the end of anticancer therapy [3]. Thus, there is a need to prevent VIPN, improve the tolerability of drugs, and maintain cancer patients' quality of life.

Peripheral nerves are composed of nerve fascicles containing bundles of nerve fibers, the perineurium, which surrounds the nerve fascicles, and the endoneurium, which is the interstitium within nerve fibers. The endoneurium contains endoneurial vessels that supply oxygen, nutrients, cytokines, drugs, and other compounds to adjacent nerves, thereby maintaining homeostasis in the microenvironment of peripheral nerves. Endoneurial vessels minimize the diffusion of drugs and other compounds that are harmful to nerves [4]. These endoneurial vessels, together with the perineurium, are called the blood–nerve barrier (BNB), which has a role in protecting peripheral nerves similar to cerebral capillaries, which form the blood–brain barrier (BBB) that protects the brain [4]. Recently, the structural and functional importance of the BNB in diabetic peripheral neuropathy and autoimmune peripheral neuropathy has been reported [5]. The BNB is closely involved in the development and progression of diabetic peripheral neuropathy due to increased vascular permeability and inflammatory cell infiltration.

The endothelial glycocalyx (eGCX) is an intracellular structure of

* Corresponding author. Department of Tumor Pathology, Gifu University Graduate School of Medicine, 1-1 Yanagido, Gifu, 501-1194, Japan.
** Corresponding author. Department of Emergency and Disaster Medicine, Gifu University Graduate School of Medicine, 1-1 Yanagido, Gifu, 501-1194, Japan.
E-mail addresses: tomita.hiroyuki.y6@f.gifu-u.ac.jp (H. Tomita), okada.hideshi.a4@f.gifu-u.ac.jp (H. Okada).
[1] These authors contributed equally to this work.

https://doi.org/10.1016/j.bbrc.2023.149286
Received 10 November 2023; Accepted 16 November 2023
Available online 21 November 2023

endothelial cells that performs several functions necessary for vascular homeostasis, including the regulation of vascular permeability, inhibition of microvascular thrombosis, and regulation of leukocyte adhesion and migration [6]. In the brain, the eGCX has been suggested to protect nerves, astrocytes, and other cells from toxins and substances released from capillaries [7]. Shedding of the eGCX is one factor that increases the permeability of the BBB [8]. However, the protective function of the eGCX as the BNB for peripheral nerves is not clear.

We hypothesized that drug-induced peripheral neuropathy may involve the leakage of anticancer drugs from endoneurial vessels that act as the BNB. Furthermore, we hypothesized that this could be prevented if the eGCX in the endoneurial vessels could be protected, preventing the increase in vascular permeability. In this study, we investigated whether vincristine disrupted the vascular eGCX and increased vascular permeability, as well as examining whether VIPN could be prevented by protecting the eGCX.

2. Materials and methods

2.1. Animals

Male C57BL6/J mice were obtained at 6 weeks of age from Charles River Japan (Kanagawa, Japan) and allowed to acclimatize for 1 week before the start of the experiments. The animals were kept in a normal light/dark cycle at 22 ± 1 °C and given a normal diet (CE-2, CLEA Japan, Inc.) and autoclaved tap water. All animal experiments were performed in accordance with the guidelines of the Gifu University International Animal Care and Use Committee (no. 2021–108, 2022–039). All behavioral experiments were conducted in the same room and in a randomized order before and after drug treatment.

2.2. Drug administration

We used 7-week-old male C57BL6/J mice (n = 8 per group). The mice were randomly assigned to four groups: no-treatment control group (G1), vincristine alone group (G2), nafamostat alone group (G3), and nafamostat treatment group (G4). Nafamostat mesylate and vincristine sulfate were purchased from Wako (Osaka, Japan). Vincristine (0.01 mg/mL, dissolved in 0.9 % saline, 0.1 mg/kg/day) and nafamostat (0.02 mg/mL, dissolved in 5 % dextrose, 0.2 mg/kg/day) were administered by intraperitoneal injection until tissues were dissected. Vincristine doses were used as previously described for VIPN models [9]. In addition, the nafamostat dose was used at the dose used in clinical practice [10].

2.3. Animal behavioral tests

To evaluate mechanical allodynia in each group, the von Frey test was used. Mechanical hypersensitivity thresholds were determined using manual von Frey filaments. In brief, each animal was placed in a Plexiglas chamber on an elevated mesh and acclimatized for at least 30 min. Mechanical force was applied in increasing amounts to the ventral surface of the hind paw until the subject demonstrated a paw withdrawal response, whereby the force was expressed in grams for each mouse at the indicated times.

To evaluate thermal allodynia in each group, the hot plate test was used and performed manually on individual animals. The manual hot plate test was performed by placing an animal on a heated surface maintained at 55 ± 1 °C. To prevent the animal from moving off the platform, a clear plastic cylinder was placed around the animal. After a brief period, typically several seconds, an animal would lift and lick a paw as the heat of the surface became uncomfortable. The animal was then immediately removed from the apparatus. The time was manually recorded by use of a stopwatch. Some mice may jump or vocalize and these responses may also be used in place of paw licking. A cut-off time, generally 30 s, must be established to minimize the risk of an animal sustaining tissue injury from prolonged exposure to the heated surface [11].

2.4. Tissue preparation

After anesthesia, the thoraxes of mice were opened, and the inferior vena cava was incised. Perfusion washing using a drip infusion system was performed with equal volumes of cold 0.1 M phosphate-buffered saline (PBS) and cold 4 % paraformaldehyde solution. The tissues were dissected, divided into pieces, and used for preparing paraffin sections.

2.5. Histological and immunohistochemical procedures

Paraffin blocks were cut into 3-μm thick sections and subjected to hematoxylin and eosin (H&E) staining as a routine procedure. Adjacent serial sections were subjected to immunohistochemistry for CD31 and PGP9.5. For immunostaining, deparaffinized sections were subjected to autoclave boiling in 0.015 M sodium citrate buffer solution (pH 6.0) for 10 min at 110 °C as an antigen retrieval procedure before incubation with 3 % H_2O_2 diluted in methanol for 10 min and blocked with 2 % normal bovine serum.

Sections were incubated with rat anti-CD31 antibody (dilution 1:50, Dianova, DIA-310) or rabbit anti-PGP9.5 antibody (dilution 1:200, Dako, Z5116) overnight at 4 °C, followed by incubation with peroxidase-labeled anti-rat or rabbit antibody (Histofine Simplestain Max PO (R); Nichirei) for 60 min at 37 °C. Immunoreaction was visualized using 3,3′-diaminobenzidine tetrahydrochloride (DAB, Sigma). The sections were counterstained with hematoxylin, mounted on slides with mounting media, and topped with coverslips.

2.6. Quantification of intraepidermal nerve fibers

Paraffin sections of mouse paws subjected to immunohistochemistry for PGP9.5 were used to evaluate the intraepidermal nerve fiber (IENF) density. IENF in each paw section were counted under 40 × magnification in a blinded fashion, and the density of the fibers was calculated as fibers/mm. Then, the mean IENF density (n = 6 per group) was calculated [12,13].

2.7. Evaluation of vascular permeability

A 2 % solution of Evans Blue (Tokyo Chemical Industry) in normal saline (4 mL/kg of body weight) was injected into the jugular vein. The stain was allowed to circulate for 16 h. Prior to sacrifice, the mice were perfused with ice-cold PBS to wash out the Evans blue solution from vessel lumens. After sacrifice, paws of a similar size were collected, and tissue samples were placed in tubes. Thereafter, 500 μl of formamide was added to each tube, and the samples were incubated at 60 °C for an additional 24 h to extract the Evans blue from tissues. Following the Evans blue extraction, the absorbance of the solution at 620 nm was measured with a 2014 EnVision Multilabel Plate Reader (PerkinElmer) [14].

2.8. Scanning and transmission electron microscopy

Sample preparation for electron microscopy was performed as described previously [15]. Briefly, to detect the microstructure of eGCX by electron microscopy, mice were anesthetized and perfused with a solution composed of 2 % glutaraldehyde, 2 % sucrose, 0.1 M sodium cacodylate buffer (pH 7.3), and 2 % lanthanum nitrate. Paws were soaked overnight in a solution without glutaraldehyde before being washed in alkaline (0.03 mol/L NaOH) sucrose (2 %) solution. The specimens were then dehydrated through a series of graded ethanol concentrations. After the *tert*-butyl alcohol had solidified, it was freeze-dried, and the specimens were examined using SEM (S-4500;

Hitachi).

To prepare samples for transmission electron microscopy, each specimen was embedded in epoxy resin. The blocks were cut at a thickness of 500 nm. Semi-thin sections were mounted on cover glass slides and incubated at 100 °C after staining with 0.1 % toluidine blue in 0.1 M phosphate buffer. Ultrathin sections (90 nm) stained with uranyl acetate and lead citrate were then examined using TEM (HT-7800; Hitachi).

2.9. Quantitative assessment of electron microscopy

All ultrastructural quantifications were performed using ImageJ software (National Institutes of Health, Bethesda). Quantitative morphometric analyses were performed on coded samples by an examiner masked to the pathology of the peripheral neuropathy. Assessments of the eGCX occupation area and the corresponding inner diameter of the capillary were performed on six capillary vessels randomly chosen from the electron microscopy images collected from each mouse [15]. Analyses of the distance between the perineurium and myelinated axons were performed on 10 myelinated axons randomly chosen from the electron microscopy images. For each case, the minimum distance between the perineurium and myelin myelinated axons was measured manually [16]. To evaluate demyelinated axons, the G-ratio (axon diameter relative to nerve fiber [axon + myelin sheath] diameter) was used [17]. Twelve myelinated axons were randomly selected for each case.

2.10. Statistical analyses

For mouse experiments, statistical details of the experiments can be found in the figure legends. Statistical significance was determined using the Student's *t*-test. For multiple comparisons, Bonferroni correction was used. All statistical analyses were performed using JMP 14.2 software (SAS Institute Inc.). Statistical significance was set at $P < 0.05$ for all analyses. All data are presented as the means ± standard error of the means.

3. Results

3.1. Suppression of VIPN by nafamostat in behavioral tests

To identify the peripheral nerves in the subcutaneous skin of mice, we analyzed the histological features microscopically (Fig. S1). Next, to investigate whether VIPN can be suppressed by eGCX protection, we established a mouse model of VIPN, which was treated with nafamostat, a candidate drug to protect the eGCX [18]. The von Frey test revealed a significant difference in the withdrawal threshold between the G2 and G1, the G2 and G3, and between the G2 and G4 after 3 weeks of vincristine administration (Fig. 1A). Similarly, the hot plate test showed a significant difference in the reaction time of mice between the G2 and G1, between the G2 and G3, and between the G2 and G4 (Fig. 1B).

3.2. Nafamostat protects the loss of intraepidermal nerve fibers in VIPN

The loss of IENF is associated with drug-induced peripheral neuropathy and changes in IENF likely occur in human VIPN [12]. Therefore, we analyzed the density of IENF in the front and hind paws of mice by immunostaining of the neuronal marker PGP9.5 (Fig. 2A). The density of IENF in the front paws was significantly lower in G2 than in G1 (1.98 ± 0.95 mm in G2 vs 10.85 ± 1.01 mm in G1) and in G4 (1.98 ± 0.95 mm in G2 vs 12.84 ± 0.75 mm in G4) (Fig. 2A and B). Similarly, the density of IENF in the hind paws was significantly lower in G2 than in G1 (2.95 ± 1.09 mm in G2 vs 8.67 ± 1.69 mm in G1) and in G4 (2.95 ± 1.09 mm in G2 vs 11.45 ± 2.51 mm in G4) (Fig. 2A, C). The density of IENF in the front and hind paws was no significant difference between the G1 and G4 (Fig. 2A–C) and between the G1 and G3 (data not shown).

3.3. Nafamostat prevents vincristine-induced axonal degeneration of nerve fibers

Drug-induced peripheral neuropathy caused by vincristine is pathologically classified as axonopathy [13]. Thus, we analyzed peripheral nerves within the perineurium by electron microscopy to determine whether nafamostat prevented the axonal degeneration of nerve fibers. Some myelinated axons in G2 exhibited morphological signs of axonal degeneration and myelinated axons appeared less densely packed (Fig. 2D). Axonal degeneration was assessed using the G-ratio (axon diameter relative to nerve fiber [axon + myelin sheath] diameter) [17]. The G-ratio was lower in G2 than in G1 and G4. There was no significant difference in the G-ratio between the G1 and G4 (Fig. 2E). There was no significant difference in the G-ratio between the G1 and G3 (data not shown).

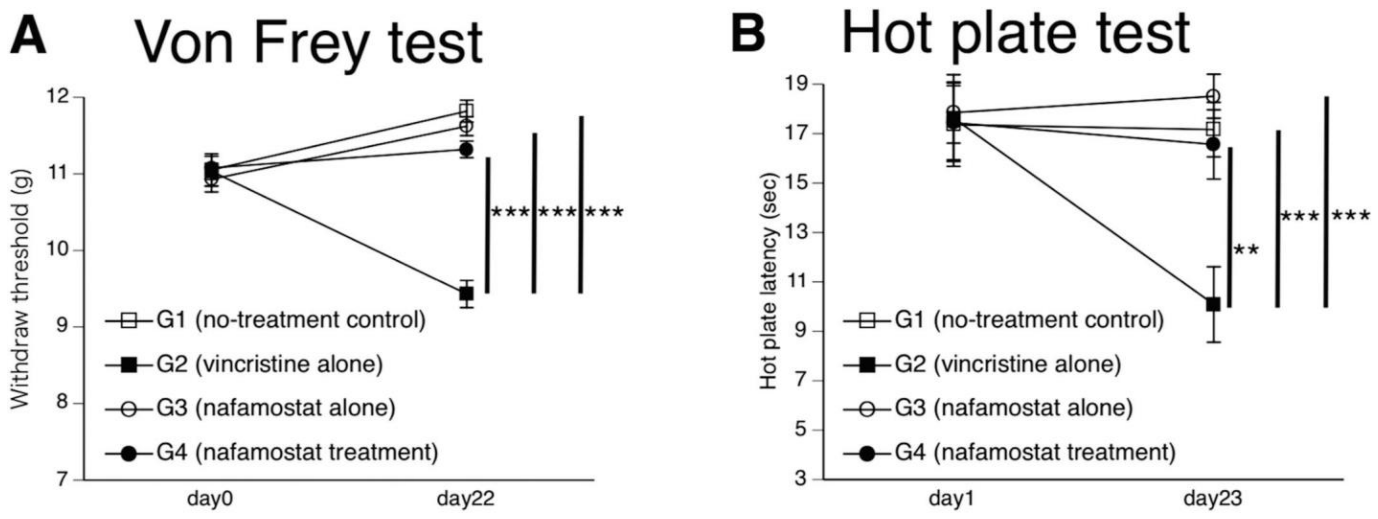

Fig. 1. Behavioral changes in vincristine-treated mice by nafamostat administration.
In the von Frey test **(A)** and hot plate test **(B)**, there was a significant difference after 3 weeks of treatment between the vincristine alone group (G2) and no-treatment control group (G1), between the G2 and nafamostat alone group (G3), and between the G2 and nafamostat treatment group (G4). Data are expressed as the means ± standard error of the means. **P < 0.01, ***P < 0.001 (Student's *t*-test corrected by the Bonferroni method).

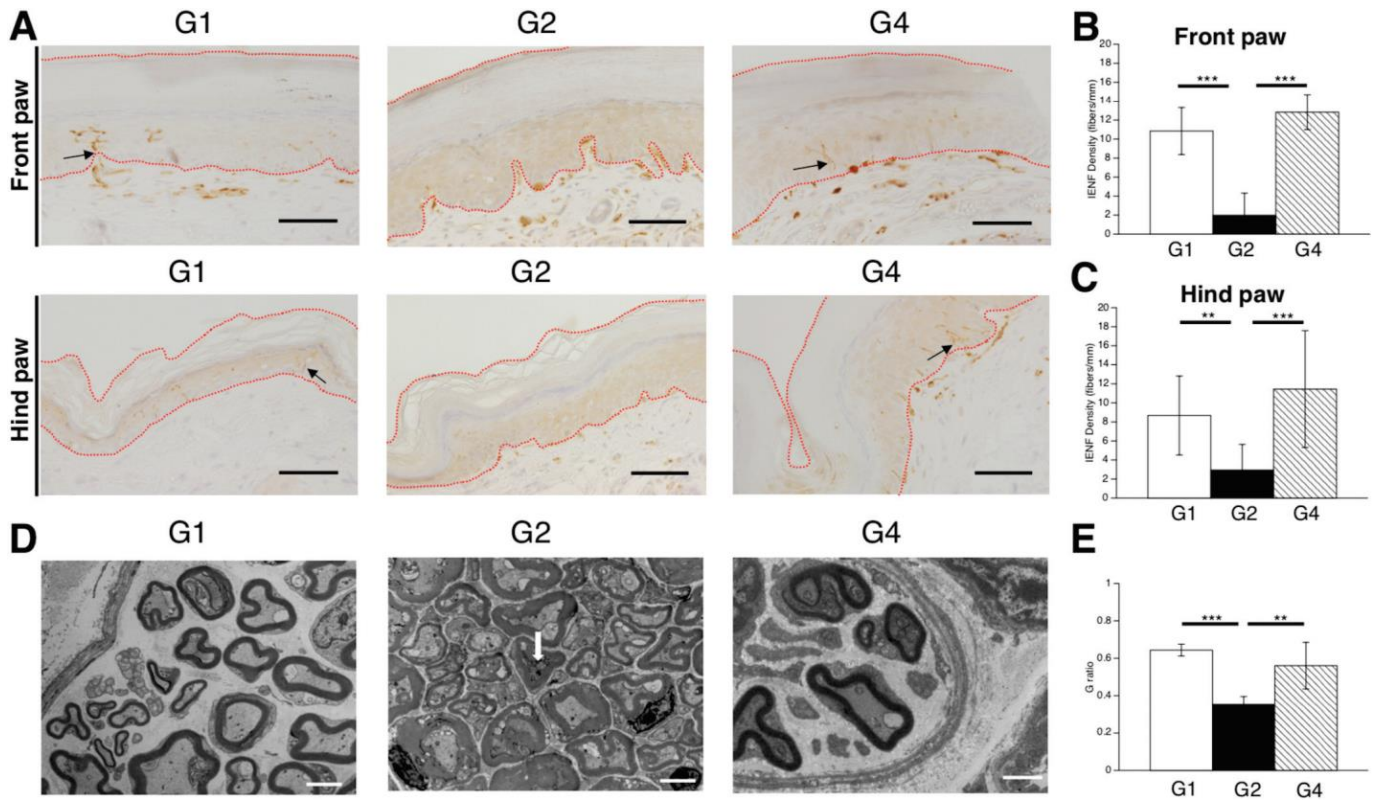

Fig. 2. Nafamostat protects against the loss of intraepidermal nerve fibers and the degeneration of myelinated axons in the paws of vincristine-treated mice. **(A)** Representative images of immunohistochemistry of PGP9.5 expression in subcutaneous tissue sections of front and hind paw specimens in the no-treatment control group (G1), vincristine alone group (G2), and nafamostat treatment group (G4) mice. Scale bars = 40 μm. Images of G1 and G4 show nerve fibers entering the epidermis (black arrows). However, few nerve fibers are entering the epidermis in G2. Red dotted lines indicate skin epidermis lesions. **(B–C)** Quantification of intraepidermal nerve fiber (IENF) density in front and hind paws (n = 6 each). The G2 had a lower IENF density than G1 and G4. **(D)** Representative transmission electron microscopy images of peripheral nerves from the G1, G2, and G4 groups. Scale bars = 30 μm. (G1) Myelinated axons had a normal structure and morphology. The integrity of the myelin sheath was normal and lined up in order. (G2) Axonal degeneration was observed (white arrow). The myelin sheath showed swelling and deformation (arrowhead). (G4) The normal structure of myelinated axons was almost preserved. Slightly less axonal damage was observed in G4 than in G2. **(E)** The graph shows the G-ratio for the G1, G2, and G4. G-ratios were calculated as the axon diameter/myelin diameter. The G2 had a lower G-ratio than the G1 and G4 groups (n = 12 each). Data are expressed as the means ± standard error of the means. **P < 0.01, ***P < 0.001 (Student's *t*-test corrected by the Bonferroni method). (For interpretation of the references to colour in this figure legend, the reader is referred to the Web version of this article.)

3.4. Nafamostat suppresses vincristine-induced edema related to vascular permeability

Anticancer drug side effects may be attributed to an in the increase vascular permeability of tissues outside the target site [19]. To determine whether VIPN is associated with vascular permeability in peripheral nerves, we analyzed Evans blue leakage in mouse paws and edema formation around nerve fibers. Our findings indicated that the G2 exhibited more Evans blue leakage compared with G1 and G4 (Fig. 3A). There was no significant difference in Evans blue leakage between the G1 and G4. There was no significant difference in the leakage between G1 and G3 (data not shown).

Furthermore, the assessment of edema formation within the endoneurium, i.e., the distance between the perineurium and myelinated fibers (Fig. 3B), was evaluated. The distance between the perineurium and myelinated fibers was 2.83 ± 3.6 μm, 39.71 ± 3.6 μm, and 16.39 ± 3.6 μm in G1, G2, and G4, respectively. This result revealed that the G2 had a greater distance than the G1 and the G4 (Fig. 3C and D). There was also a significant difference in the distance between the G1 and G4. There was no significant difference in the distance between the G1 and G3 (data not shown).

3.5. Potential involvement of eGCX protection by nafamostat in preventing VIPN

The eGCX is thought to regulate vascular permeability and the homeostasis of endothelial cells [7,8]. To clarify the status of the eGCX in VIPN and to investigate whether nafamostat prevents its shedding in VIPN, we observed the eGCX by electron microscopy.

Transmission electron microscopy showed a moss-like eGCX, which covered the endothelium, in the lumen of capillary vessels (Fig. 4A). The G1 and G4 had a rich eGCX covering the endoneurium, but the G2 had very few eGCX (Fig. 4A). The percentage of the eGCX covering the vascular lumen was significantly higher in the G1 (33.53 ± 7.06 %) and G4 (36.12 ± 7.06 %) compared with the G2 (3.73 ± 7.06 %) (Fig. 4B). There was no significant difference in the percentage of the eGCX covering the vascular lumen between the G1 and G4.

Scanning electron microscopy, which can show three-dimensional images, showed that the eGCX covered the endothelium in the G1 and G4. However, in the G2, the eGCX did not cover the endothelium (Fig. 4C).

4. Discussion

Morphological changes of the eGCX and their involvement in the pathogenesis of chronic diseases such as diabetes, hypertension, and cancer as well as in acute diseases such as sepsis and trauma have

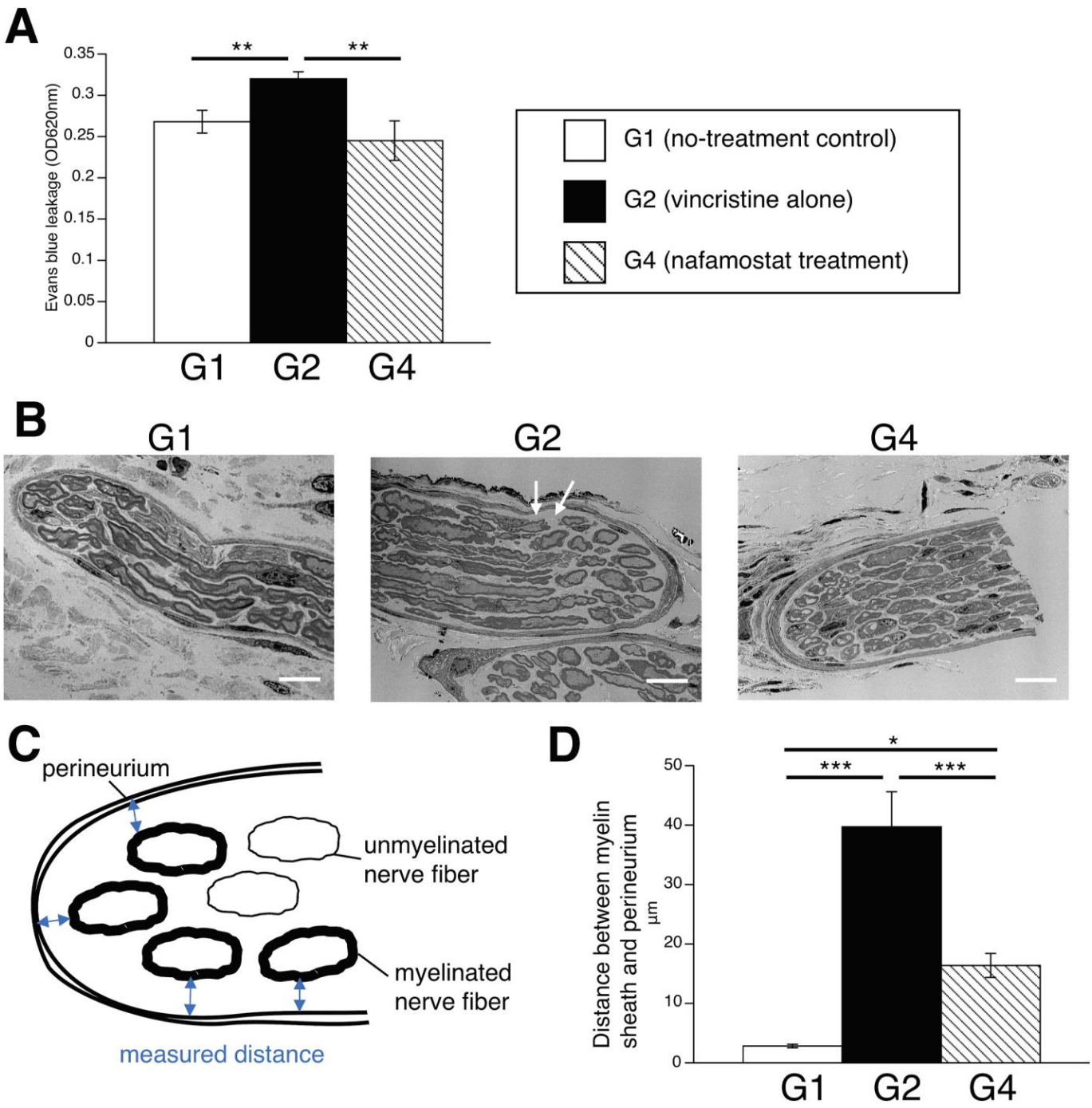

Fig. 3. Nafamostat decreases the vascular permeability in the paws of vincristine-treated mice.
(A) The graph shows the leakage of Evans blue in the paws of mice. The vincristine alone group (G2) had more Evans blue leakage than the no-treatment control group (G1) and nafamostat treatment group (G4) (n = 3 each). **(B)** Representative transmission electron microscopy images of peripheral nerves from the G1, G2, and G4 groups. Scale bars = 80 μm. The white arrow in G2 indicates edema formation in the endoneurium. **(C)** Schematic diagram of the assessment method of the distance between the perineurium and myelinated fibers. **(D)** The graph shows the minimum distance between the perineurium and myelinated axons in transmission electron microscope images. The G2 had a longer distance than the G1 and G4 groups (n = 10 each). Data are expressed as the means ± standard error of the means. *P < 0.05, **P < 0.01, ***P < 0.001 (Student's *t*-test corrected by the Bonferroni method). (For interpretation of the references to colour in this figure legend, the reader is referred to the Web version of this article.)

attracted much attention [20]. However, no studies have reported an association between drug-induced peripheral neuropathy and the eGCX. Our current study suggests that protecting the eGCX may prevent VIPN. Our knowledge of the eGCX is accumulating, and it is thought to have an important function in the BBB [7]. It has been suggested that inhibiting eGCX shedding may protect the brain. However, unlike the brain, peripheral nerves are not surrounded by astrocytes, although they do share similarities regarding capillaries [21]. Both have strong vascular endothelial cell adhesion that protects nerves by preventing the diffusion of potentially neuropathic substances [4,21]. In diabetic peripheral neuropathy and other peripheral neuropathies, damage to the endoneurial vessels has been proposed as a key etiological factor [5,22]. This damage involves endothelial injury leading to the disruption of tight junctions, pericyte loss, and endothelial hypertrophy [5]. The present study

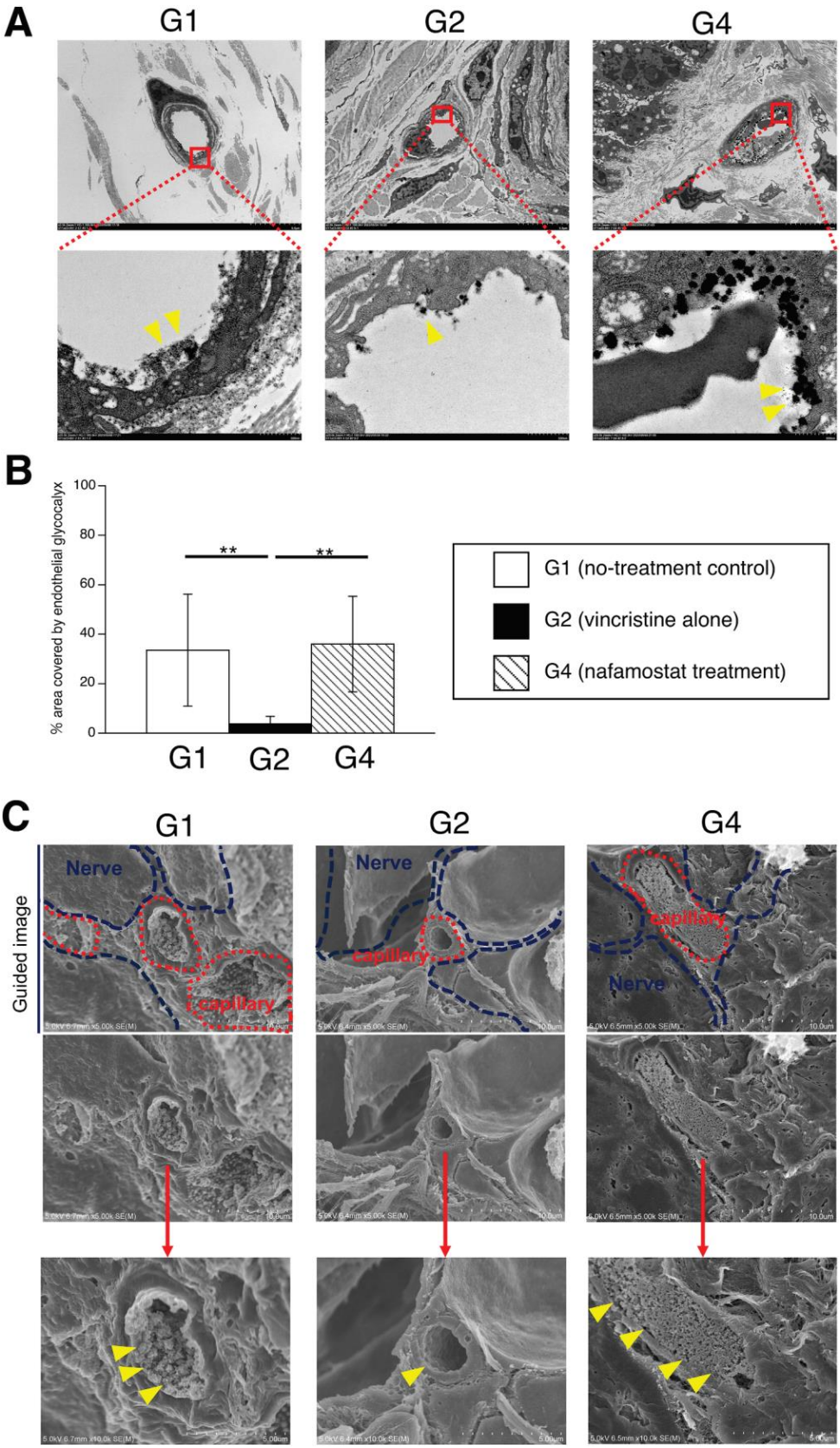

(caption on next page)

Fig. 4. Nafamostat suppresses the disruption of the endothelial glycocalyx in the paws of vincristine-treated mice.
(A) Representative transmission electron microscopy images in the no-treatment control (G1), vincristine alone (G2), and nafamostat treatment (G4) groups. The endothelial glycocalyx (eGCX) covered the endothelium in the G1 and G4. However, shedding of the eGCX was observed in the G2. Arrow heads indicate the eGCX. **(B)** The graph shows the percentage of the eGCX covering the vessel lumen in transmission electron microscopy images. The percentage of the eGCX covering the vessel lumen was greater in the G1 and G4 groups than in the G2 (n = 6 each). Data are expressed as the means ± standard error of the means. **P < 0.01 (Student's *t*-test corrected by the Bonferroni method). **(C)** Representative scanning electron microscopy images in the G1, G2, and G4 groups. (*Upper*) In the guide image, blue dotted lines indicate peripheral nerves and red dotted lines indicate capillaries. (*Lower*) In the G1 and G4 groups, the eGCX near the peripheral nerves covered the endothelium. However, the eGCX did not cover the endothelium in the G2. Arrow heads indicate the eGCX. (For interpretation of the references to colour in this figure legend, the reader is referred to the Web version of this article.)

demonstrates that in addition to these endothelial disorders, drug-induced peripheral neuropathy involves eGCX shedding. This emphasizes the potentially significant role of the eGCX in peripheral nerves, paralleling its role in the BBB [7].

Previous studies observed the microenvironment of peripheral nerves in neuropathy and reported the presence of edema and increased vascular permeability within the endoneurium [16,23]. Our current study provides evidence supporting the involvement of eGCX shedding and increased vascular permeability in the pathogenesis of VIPN. Anticancer drugs primarily exert their anticancer effects upon reaching the target site via the bloodstream. However, these drugs can also lead to side effects when they unintentionally reach non-target tissues. Preventing these drugs from escaping the confines of blood vessels is a logical approach to mitigate these side effects [19]. Together, eGCX shedding and the leakage of anti-tumor drugs to peripheral nerves may also contribute to the development of drug-induced peripheral neuropathy.

There were several limitations in this study. First, the precise mechanisms by which nafamostat achieves eGCX protection remain unclear. It is postulated that nafamostat functions by suppressing inflammation, which contributes to eGCX damage [10,24]. Further research is required to ascertain how nafamostat may confer protection to the eGCX in chemotherapy-induced peripheral neuropathy, including whether it exerts a specific glycocalyx-neoplastic effect. Second, the eGCX is a complex structure composed of multiple glycans and glycoproteins, and hyaluronan [6]. Hyaluronan is thought to primarily regulate vascular permeability [25], yet it remains unclear which specific elements are most affected by vincristine and protected by nafamostat. Subsequent studies are expected to advance the prevention of drug-induced peripheral neuropathy with a specific focus on the eGCX.

Our findings suggested that nafamostat, an eGCX-protecting drug, may prevent VIPN by inhibiting vascular permeability. The drug repositioning of nafamostat for this purpose might allow for its quick approval for use in human patients. eGCX protection is a potential new therapeutic strategy for the prevention of drug-induced peripheral neuropathy.

CRediT authorship contribution statement

Kazufumi Ohmura: Data curation, Formal analysis, Investigation, Validation, Visualization, Writing – original draft. **Takamasa Kinoshita:** Conceptualization, Investigation, Writing – review & editing. **Hiroyuki Tomita:** Conceptualization, Data curation, Funding acquisition, Project administration, Resources, Supervision, Writing – original draft. **Hideshi Okada:** Conceptualization, Investigation, Methodology, Project administration, Writing – review & editing. **Masayoshi Shimizu:** Investigation, Methodology, Writing – review & editing. **Kosuke Mori:** Investigation, Methodology, Writing – review & editing. **Toshiaki Taniguchi:** Data curation, Investigation, Writing – review & editing. **Akio Suzuki:** Data curation, Investigation, Writing – review & editing. **Toru Iwama:** Supervision, Writing – review & editing, Resources. **Akira Hara:** Funding acquisition, Resources, Writing – review & editing, Project administration.

Declaration of competing interest

All authors declare no conflicts of interest.

Acknowledgment

We would like to thank Kyoko Takahashi, Ayako Suga, Chihiro Takada, Reiko Kitazumi for their experimental support. This study was supported by JSPS KAKENHI JP20K0758723 (H.T.), JP23H03326 (H.T.), JP23K06276 (A.S.), and JST FOREST Program JPMJFR220W (H.T.).

Appendix A. Supplementary data

Supplementary data to this article can be found online at https://doi.org/10.1016/j.bbrc.2023.149286.

References

[1] S. Triarico, A. Romano, G. Attinà, et al., Vincristine-induced peripheral neuropathy (VIPN) in pediatric tumors: mechanisms, risk factors, strategies of prevention and treatment, Int. J. Mol. Sci. 22 (2021) 4112.
[2] Q.Y. Yang, Y.H. Hu, H.L. Guo, et al., Vincristine-induced peripheral neuropathy in childhood acute lymphoblastic leukemia: genetic variation as a potential risk factor, Front. Pharmacol. 12 (2021), 771487.
[3] N. Haim, R. Epelbaum, M. Ben-Shahar, et al., Full dose vincristine (without 2-mg dose limit) in the treatment of lymphomas, Cancer 73 (1994) 2515–2519.
[4] Y. Olsson, Microenvironment of the peripheral nervous system under normal and pathological conditions, Crit. Rev. Neurobiol. 5 (1990) 265–311.
[5] M. Richner, N. Ferreira, A. Dudele, et al., Functional and structural changes of the blood-nerve-barrier in diabetic neuropathy, Front. Neurosci. 12 (2019) 1038.
[6] O. Yilmaz, B. Afsar, A. Ortiz, et al., The role of endothelial glycocalyx in health and disease, Clin Kidney J 12 (2019) 611–619.
[7] F. Zhao, L. Zhong, Y. Luo, Endothelial glycocalyx as an important factor in composition of blood-brain barrier, CNS Neurosci. Ther. 27 (2021) 26–35.
[8] G. Guven, M.P. Hilty, C. Ince, Microcirculation: physiology, pathophysiology, and clinical application, Blood Purif. 49 (2020) 143–150.
[9] M. Khodaei, S. Mehri, S.R. Pour, et al., The protective effect of chemical and natural compounds against vincristine-induced peripheral neuropathy (VIPN), Naunyn-Schmiedeberg's Arch. Pharmacol. 395 (2022) 907–919.
[10] X. Chen, Z. Xu, S. Zeng, et al., The molecular aspect of antitumor effects of protease inhibitor nafamostat mesylate and its role in potential clinical applications, Front. Oncol. 9 (2019) 852.
[11] A.W. Bannon, A.B. Malmberg, Models of nociception: hot-plate, tail-flick, and formalin tests in rodents, Curr Protoc Neurosci 41 (2007) 8–9.
[12] S. Geisler, R.A. Doan, A. Strickland, et al., Prevention of vincristine-induced peripheral neuropathy by genetic deletion of SARM1 in mice, Brain 139 (2016) 3092–3108.
[13] S.B. Park, A. Cetinkaya-Fisgin, A.A. Argyriou, et al., Axonal degeneration in chemotherapy-induced peripheral neurotoxicity: clinical and experimental evidence, J. Neurol. Neurosurg. Psychiatry 94 (2023) 962–972.
[14] S.H. Lee, H. J Shin, D.Y. Kim, et al., Streptochlorin suppresses allergic dermatitis and mast cell activation via regulation of Lyn/Fyn and Syk signaling pathways in cellular and mouse models, PLoS One 8 (2013), e74194.
[15] H. Okada, G. Takemura, K. Suzuki, et al., Three-dimensional ultrastructure of capillary endothelial glycocalyx under normal and experimental endotoxemic conditions, Crit. Care 21 (2017) 261.
[16] N. Üçeyler, G. Necula, E. Wagemann, et al., Endoneurial edema in sural nerve may indicate recent onset inflammatory neuropathy, Muscle Nerve 53 (2016) 705–710.
[17] K. J Pollard, B. Bolon, M. J Moore, Comparative analysis of chemotherapy-induced peripheral neuropathy in bioengineered sensory nerve tissue distinguishes mechanistic differences in early-stage vincristine-, cisplatin-, and paclitaxel-induced nerve damage, Toxicol. Sci. 180 (2021) 76–88.
[18] N. Sagawa, Y. Oshima, T. Hiratsuka, et al., Role of increased vascular permeability in chemotherapy-induced alopecia: in vivo imaging of the hair follicular microenvironment in mice, Cancer Sci. 111 (2020) 2146–2155.
[19] K. Kusuzawa, K. Suzuki, H. Okada, et al., Measuring the concentration of serum syndecan-1 to assess vascular endothelial glycocalyx injury during hemodialysis, Front. Med. 8 (2021), 791309.

[20] S. Ghasempour, S.A. Feeman, The glycocalyx and immune evasion in cancer, FEBS J. 290 (2023) 55–65.
[21] J.A. Kiernan, Vascular permeability in the peripheral autonomic and somatic nervous systems: controversial aspects and comparisons with the blood-brain barrier, Microsc. Res. Tech. 35 (1996) 122–136.
[22] A.K. Reinhold, H.L. Rittner, Characteristics of the nerve barrier and the blood dorsal root ganglion barrier in health and disease, Exp. Neurol. 327 (2020), 113244.
[23] M.S. Bush, A.R. Reid, G. Allt, Blood-nerve barrier: ultrastructural and endothelial surface charge alterations following nerve crush, Neuropathol. Appl. Neurobiol. 19 (1993) 31–40.
[24] M.A. Alberelli, D.E. Candia, Functional role of protease activated receptors in vascular biology, Vasc. Pharmacol. 62 (2014) 72–81.
[25] A.R. Pries, T.W. Secomb, P. Gaehtgens, The endothelial surface layer, Pflügers Archiv 440 (2000) 653–666.